4 van den Boom R, Lesnik Oberstein SA, Spilt A, Behloul F, Ferrari MD, Haan J, Westendorp RG, van Buchem MA: Cerebral hemodynamics and white matter hyperintensities in CADASIL. J Cereb Blood Flow Metab 2003;23:599–604.
5 Chabriat H, Pappata S, Ostergaard L, Clark CA, Pachot-Clouard M, Vahedi K, Jobert A, Le Bihan D, Bousser MG: Cerebral hemodynamics in CADASIL before and after acetazolamide challenge assessed with MRI bolus tracking. Stroke 2000;31:1904–1912.
6 Mellies JK, Baumer T, Muller JA, Tournier-Lasserve E, Chabriat H, Knobloch O, Hackeloer HJ, Goebel HH, Wetzig L, Haller P: Spect study of a German CADASIL family: a phenotype with migraine and progressive dementia only. Neurology 1998;50:1715–1721.
7 Pfefferkorn T, von Stuckrad-Barre S, Herzog J, Gasser T, Hamann GF, Dichgans M: Reduced cerebrovascular CO(2) reactivity in CADASIL: a transcranial Doppler sonography study. Stroke 2001;32:17–21.
8 Ruchoux MM, Domenga V, Brulin P, Maciazek J, Limol S, Tournier-Lasserve E, Joutel A: Transgenic mice expressing mutant notch3 develop vascular alterations characteristic of cerebral autosomal dominant arteriopathy with subcortical infarcts and leukoencephalopathy. Am J Pathol 2003;162:329–342.
9 Dubroca C, Lacombe P, Domenga V, Maciazek J, Levy B, Tournier-Lasserve E, Joutel A, Henrion D: Impaired vascular mechanotransduction in a transgenic mouse model of CADASIL arteriopathy. Stroke 2005;36:113–117.
10 Ruchoux MM, Chabriat H, Bousser MG, Baudrimont M, Tournier-Lasserve E: Presence of ultrastructural arterial lesions in muscle and skin vessels of patients with CADASIL. Stroke 1994;25:2291–2292.
11 Ruchoux MM, Maurage CA: Endothelial changes in muscle and skin biopsies in patients with CADASIL. Neuropathol Appl Neurobiol 1998;24:60–65.
12 Stenborg A, Kalimo H, Viitanen M, Terent A, Lind L: Impaired endothelial function of forearm resistance arteries in CADASIL patients. Stroke 2007;38:2692–2697.
13 Peters N, Freilinger T, Opherk C, Pfefferkorn T, Dichgans M: Enhanced L-arginine-induced vasoreactivity suggests endothelial dysfunction in CADASIL. J Neurol 2008; 255:1203–1208.
14 Mawet J, Vahedi K, Aout M, Vicaut E, Duering M, Touboul PJ, Dichgans M, Chabriat H: Carotid atherosclerotic markers in CADASIL. Cerebrovasc Dis 2010;31:246–252.
15 Gobron C, Vahedi K, Vicaut E, Stucker O, Laemmel E, Baudry N, Bousser MG, Chabriat H: Characteristic features of in vivo skin microvascular reactivity in CADASIL. J Cereb Blood Flow Metab 2007;27:250–257.
16 Hamburg NM, Benjamin EJ: Assessment of endothelial function using digital pulse amplitude tonometry. Trends Cardiovasc Med 2009;19:6–11.
17 Kuvin JT, Patel AR, Sliney KA, Pandian NG, Sheffy J, Schnall RP, Karas RH, Udelson JE: Assessment of peripheral vascular endothelial function with finger arterial pulse wave amplitude. Am Heart J 2003;146:168–174.
18 Kuvin JT, Mammen A, Mooney P, Alsheikh-Ali AA, Karas RH: Assessment of peripheral vascular endothelial function in the ambulatory setting. Vasc Med 2007;12:13–16.
19 Chabriat H, Levy C, Taillia H, Iba-Zizen MT, Vahedi K, Joutel A, Tournier-Lasserve E, Bousser MG: Patterns of MRI lesions in CADASIL. Neurology 1998;51:452–457.
20 Iida H, Itoh H, Nakazawa M, Hatazawa J, Nishimura H, Onishi Y, Uemura K: Quantitative mapping of regional cerebral blood flow using iodine-123-IMP and SPECT. J Nucl Med 1994;35:2019–2030.
21 Minoshima S, Koeppe RA, Frey KA, Kuhl DE: Anatomic standardization: linear scaling and nonlinear warping of functional brain images. J Nucl Med 1994;35:1528–1537.
22 Minoshima S, Frey KA, Koeppe RA, Foster NL, Kuhl DE: A diagnostic approach in Alzheimer's disease using three-dimensional stereotactic surface projections of fluorine-18-FDG PET. J Nucl Med 1995;36:1238–1248.
23 Mizumura S, Nakagawara J, Takahashi M, Kumita S, Cho K, Nakajo H, Toba M, Kumazaki T: Three-dimensional display in staging hemodynamic brain ischemia for jet study: objective evaluation using SEE analysis and 3D-SSP display. Ann Nucl Med 2004; 18:13–21.
24 Nohria A, Gerhard-Herman M, Creager MA, Hurley S, Mitra D, Ganz P: Role of nitric oxide in the regulation of digital pulse volume amplitude in humans. J Appl Physiol 2006;101:545–548.
25 Bonetti PO, Pumper GM, Higano ST, Holmes DR Jr., Kuvin JT, Lerman A: Noninvasive identification of patients with early coronary atherosclerosis by assessment of digital reactive hyperemia. J Am Coll Cardiol 2004;44:2137–2141.
26 Hamburg NM, Keyes MJ, Larson MG, Vasan RS, Schnabel R, Pryde MM, Mitchell GF, Sheffy J, Vita JA, Benjamin EJ: Cross-sectional relations of digital vascular function to cardiovascular risk factors in the Framingham heart study. Circulation 2008;117: 2467–2474.
27 Rufa A, Blardi P, De Lalla A, Cevenini G, De Stefano N, Zicari E, Auteri A, Federico A, Dotti MT: Plasma levels of asymmetric dimethylarginine in cerebral autosomal dominant arteriopathy with subcortical infarct and leukoencephalopathy. Cerebrovasc Dis 2008;26:636–640.
28 Brulin P, Godfraind C, Leteurtre E, Ruchoux MM: Morphometric analysis of ultrastructural vascular changes in CADASIL: analysis of 50 skin biopsy specimens and pathogenic implications. Acta Neuropathol (Berl) 2002; 104:241–248.
29 Lacombe P, Oligo C, Domenga V, Tournier-Lasserve E, Joutel A: Impaired cerebral vasoreactivity in a transgenic mouse model of cerebral autosomal dominant arteriopathy with subcortical infarcts and leukoencephalopathy arteriopathy. Stroke 2005;36:1053–1058.
30 Matsuzawa Y, Sugiyama S, Sugamura K, Nozaki T, Ohba K, Konishi M, Matsubara J, Sumida H, Kaikita K, Kojima S, Nagayoshi Y, Yamamuro M, Izumiya Y, Iwashita S, Matsui K, Jinnouchi H, Kimura K, Umemura S, Ogawa H: Digital assessment of endothelial function and ischemic heart disease in women. J Am Coll Cardiol 2010;55:1688–1696.

Neurologic Image

European Neurology

Eur Neurol 2013;69:352–353
DOI: 10.1159/000348720

Received: January 19, 2013
Accepted: January 28, 2013
Published online: April 26, 2013

Increasing Microbleeds in CADASIL

Takuya Yagi[a] Fumie Konoeda[a] Ikuko Mizuta[b] Toshiki Mizuno[b]
Norihiro Suzuki[a]

[a]Department of Neurology, Keio University School of Medicine, Tokyo, and [b]Department of Neurology, Kyoto Prefectural University of Medicine, Kyoto, Japan

Following left thalamic hemorrhage and several ischemic episodes, a 45-year-old male with mild hypertension and diabetes mellitus was diagnosed with CADASIL by genetic testing (fig. 1a). Despite less-characteristic evidence of CADASIL in the external capsules and the poles of the temporal lobes (fig. 1b), cerebral microbleeds increased yearly on T2* MRI (fig. 1c), indicating the pathogenesis of microbleeds in CADASIL may be independent of white matter hyperintensity lesions [1] and cerebrovascular risk factors may modulate the progression of microbleeds in CADASIL [2].

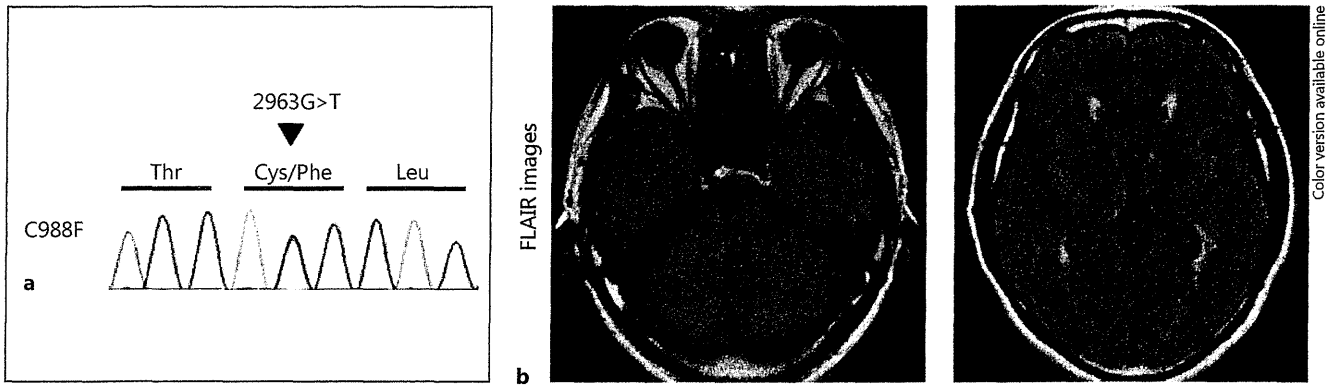

Fig. 1. a Genetic testing revealed p.Cys988Phe (C.2963G>T) mutation in exon 18 of the patient's *NOTCH3* gene. **b** FLAIR imaging at 51 years of age showed the anterior temporal poles and the external capsules appeared relatively sparse in this case as compared with typical findings of CADASIL.

0014–3022/13/0696–0352$38.00/0

E-Mail karger@karger.com
www.karger.com/ene

Dr. Takuya Yagi
Department of Neurology, Keio University School of Medicine
35 Shinanomachi, Shinjuku-ku
Tokyo 160-8582 (Japan)
E-Mail takuyagi@2006.jukuin.keio.ac.jp

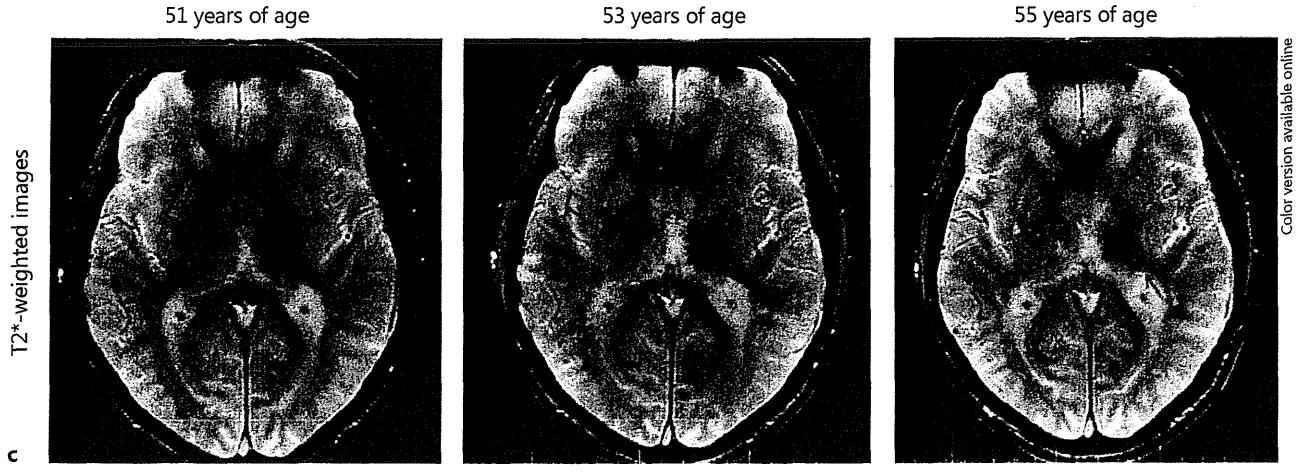

Fig. 1. c T2*-weighted imaging revealed prominent cerebral microbleeds that increased in number from year to year. Arrows point to the new microbleed lesions.

References

1 Dichgans M, Holtmannspötter M, Herzog J, Peters N, Bergmann M, Yousry TA: Cerebral microbleeds in CADASIL: a gradient-echo magnetic resonance imaging and autopsy study. Stroke 2002;33:67–71.

2 Viswanathan A, Guichard JP, Gschwendtner A, Buffon F, Cumurcuic R, Boutron C, Vicaut E, Holtmannspötter M, Pachai C, Bousser MG, Dichgans M, Chabriat H: Blood pressure and haemoglobin A1c are associated with microhaemorrhage in CADASIL: a two-centre cohort study. Brain 2006;129:2375–2383.

INTERNAL MEDICINE

□ CASE REPORT □

Early Involvement of the Corpus Callosum in a Patient with Hereditary Diffuse Leukoencephalopathy with Spheroids Carrying the *de novo* K793T Mutation of *CSF1R*

Yasufumi Kondo[1], Michiaki Kinoshita[1], Kazuhiro Fukushima[1], Kunihiro Yoshida[2] and Shu-ichi Ikeda[1]

Abstract

We herein report the case of a 41-year-old Japanese man with hereditary diffuse leukoencephalopathy with spheroids (HDLS) who carried the *de novo* K793T mutation in the colony-stimulating factor 1 receptor gene (*CSF1R*). He showed a gradual decline of his cognitive and mental functions over the following six months. On brain MRI, a thin corpus callosum with T2- and FLAIR-high signal intensity in the splenium was conspicuous, whereas cerebral deep and periventricular white matter lesions were mild. We propose that a diagnosis of HDLS should be considered in patients with presenile dementia presenting with corpus callosum lesions on MRI, even in cases with a lack of any apparent family history.

Key words: HDLS, *CSF1R*, *de novo* mutation, corpus callosum

(Intern Med 52: 503-506, 2013)
(DOI: 10.2169/internalmedicine.52.8879)

Introduction

Hereditary diffuse leukoencephalopathy with spheroids (HDLS) is an autosomal-dominant white matter disease caused by mutations in the colony-stimulating factor 1 receptor gene (*CSF1R*) (1). It is characterized clinically by adult-onset behavioral, cognitive and motor dysfunction and pathologically by a widespread loss of axons and myelin sheaths and the appearance of axonal spheroids and pigmented macrophages (2-4). Several sporadic patients who fulfill the clinical and pathological criteria for HDLS have been reported (5-8). However, it remains unknown whether these sporadic cases reflect phenotypic copies, reduced disease penetrance or are caused by *de novo* mutations in the genes responsible for the HDLS phenotype (4).

We herein describe the case of an HDLS patient who carried a novel *de novo* K793T mutation in *CSF1R*. This is the second family, next to the Norwegian family described by Rademakers et al. (1), in which both parents have been shown to not carry the causative *CSF1R* mutation. The cases of these families clearly suggest that a subset of sporadic cases of HDLS are caused by *de novo CSF1R* mutations. Furthermore, we propose that involvement of the corpus callosum on MRI may be an early diagnostic clue indicating a diagnosis of HDLS.

Case Report

A 41-year-old Japanese man had been well until 40 years of age when he began to show a decline in his cognitive function. He was first noticed to have difficulty performing occupational tasks and handling a cell phone in October 2011. In January 2012, he twice developed confusion and unresponsiveness while during drinking alcohol. His wife encouraged him to visit the hospital in February 2012, where he was suspected of having presenile dementia. Thereafter, he became unable to use a personal computer or drive a car and had to quit working. His wife noted that his speech and gait had become awkward. His previous medical history was unremarkable. There was no particular family history of psychiatric or neurological diseases. His parents

[1]Department of Medicine (Neurology and Rheumatology), Shinshu University School of Medicine, Japan and [2]Department of Brain Disease Research, Shinshu University School of Medicine, Japan
Received for publication August 28, 2012; Accepted for publication November 14, 2012
Correspondence to Dr. Kunihiro Yoshida, kyoshida@shinshu-u.ac.jp

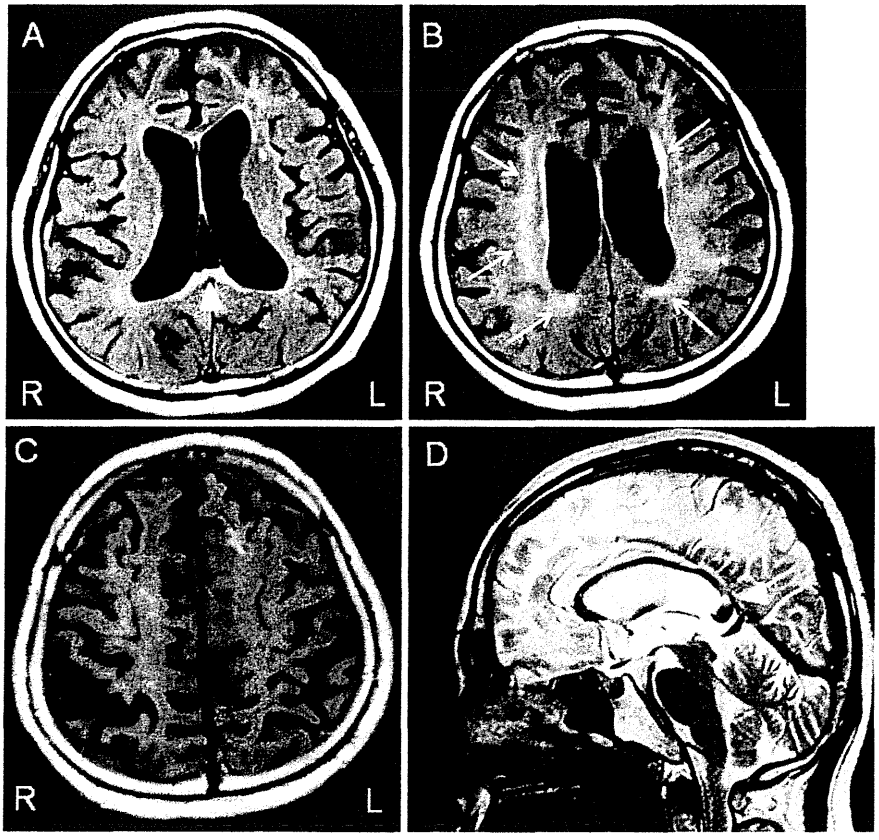

Figure 1. Brain MRI images. Brain MRI images of the patient (at 41 years of age) are shown. Dilatation of the lateral ventricles and hyperintense foci are observed in the cerebral deep and periventricular white matter on FLAIR-weighted images (arrow, A-C). The corpus callosum is atrophic and shows high signal intensity in the splenium (arrowhead) on FLAIR-weighted (A) and T2-weighted images (D).

and two sisters were healthy.

On admission in April 2012, the patient was found to be normotensive and the general findings were not particular. He was cooperative, although he did not appear to have any awareness of being ill. A neurological examination showed a slow initiation of speech, dysarthria, slight left hemiplegia and an unstable gait. The patient's deep tendon reflexes were slightly exaggerated; however, his plantar responses were flexor. No rigidity or involuntary movements were observed. The Mini-Mental State Examination score was 23 points and the Frontal Assessment Battery (FAB) score was 10 points. These tests demonstrated poor attention, calculation and comprehension and a disturbance in verbal fluency; however, the patient's short-term memory was relatively well preserved.

The routine laboratory findings were unremarkable. Tests with negative or normal results were as follows: vitamin B1, vitamin B12, anti-nuclear antibody, syphilis, HIV, soluble interleukin 2 receptor and angiotensin converting enzyme. A cerebrospinal fluid examination showed a slight increase in the levels of total protein (51 mg/dL) and tau protein (290 pg/mL, normal value: 0-200 pg/mL). Brain MRI disclosed frontoparietal lobe atrophy and ventricular dilatation with high-intensity lesions in the cerebral deep white matter (Fig. 1). Hyperintense foci were more evident in the right hemisphere than in the left. The corpus callosum was atrophic and showed high signal intensity in the splenium (Fig. 1). No microbleeds were detected in the white matter or basal ganglia on T2*-weighted images (data not shown). There was no atrophy or signal changes in the cerebellum or brainstem. Cerebral angiography showed no findings of atherosclerosis. The findings of a nerve conduction study were normal.

The clinical and neuroradiological findings reminded us of the possibility of frontotemporal dementia, leukoencephalopathy or leukodystrophy of several genetic causes, vascular dementia (VaD) (including Binswanger disease), cerebral autosomal dominant arteriopathy with subcortical infarcts and leukoencephalopathy (CADASIL), multiple sclerosis (MS) or progressive multifocal leukoencephalopathy (PML). Immediately before this patient was referred to us, we experienced another patient with leukoencephalopathy who exhibited presenile dementia and a thin corpus callosum on MRI, similar to our patient, and was diagnosed as having HDLS based on a brain biopsy and a *CSF1R* analysis (9). Therefore, we first searched for the *CSF1R* mutation after obtaining informed consent from the patient's wife and parents.

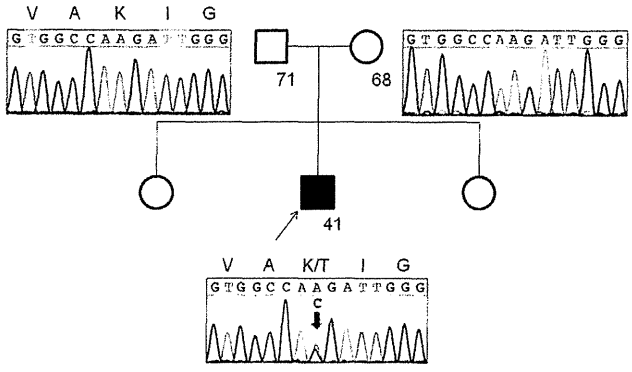

Figure 2. Molecular analysis of *CSF1R*. The sequencing results of exon 18 of *CSF1R* indicate a heterozygous c.2378A>C (p. Lys793Thr) substitution in the patient (indicated by the red arrow). The cDNA and protein numberings are relative to NM_005211.3 starting at the translation initiation codon and NP_005202.2, respectively. Neither parent has the mutation.

Genomic DNA was extracted from peripheral blood samples obtained from the patient and his parents using the Gentra Puregene Blood Kit (QIAGEN). Exons 12-22 of *CSF1R*, the mutation 'hot spots' in HDLS patients, were PCR-amplified according to a previous report (1), purified and subjected to direct sequencing. We found the p.K793T (c.2378A>C) mutation in the patient, but not in his parents (Fig. 2). Similar to the *CSF1R* mutations reported previously (1, 9), this mutation is involved in a highly conserved amino acid in the intracytoplasmic tyrosine kinase domain of *CSF1R*. An in silico analysis using PolyPhen-2 indicated that the change was probably damaging. This mutation was not detected in 80 Japanese control individuals.

Discussion

Previously, a definitive diagnosis of HDLS was made based on postmortem, neuropathological examinations only. Owing to the availability of molecular analyses of *CSF1R*, however, our patient was diagnosed as having HDLS in the early stage when he was still self-supporting at home approximately six months after the onset of symptoms.

Brain MRI, which disclosed lateral ventricle enlargement with corpus callosum lesions, was an important tool in the diagnosis of our patient. Sundal et al. reported the MRI characteristics of 15 HDLS patients with *CSF1R* mutations (10). Of these 15 patients, 14 exhibited corpus callosum involvement (the disease duration at the initial MRI study ranged from 0.5 to 5.0 years). Corpus callosum involvement included atrophy (eight patients), T2- and FLAIR-high signal intensity (11 patients) and both atrophy and signal changes in the corpus callosum (five patients) (10). In our patient, MRI performed at a disease duration of approximately six months showed atrophy and signal changes in the corpus callosum. At this stage, the cerebral deep and periventricular white matter lesions were mild and not confluent. These findings suggest that early involvement of the corpus callosum can be a diagnostic clue of HDLS.

A number of neurological diseases involving presenile dementia should be differentiated from HDLS. One of the key points for making the differential diagnosis is the regional distribution of white matter lesions. For example, white matter lesions in X-linked adrenoleukodystrophy are observed predominantly in the parietooccipital lobes (11), whereas those in HDLS are frontal dominant (10). White matter lesions in the temporal tip and external capsules are pathognomonic in CADASIL (12); however, they were not observed in seven HDLS patients, including the present patient (Kinoshita et al. unpublished observation). However, the MRI findings of HDLS closely resemble those of primary progressive MS or VaD, as they commonly show relatively symmetrical white matter lesions with corpus callosum atrophy (8, 13-15). We are now carrying out a detailed examination of the MRI characteristics of HDLS patients in comparison with those of VaD patients (Kinoshita et al. manuscript in preparation).

The patient was sporadic with both parents being healthy until their late sixties or early seventies. The mode of inheritance of HDLS is autosomal-dominant; however, several sporadic patients who met the clinical and neuropathological criteria for HDLS have been reported (5-8). Such patients might be reported under a diagnosis of pigmentary orthochromatic leukodystrophy (POLD), which shows quite similar clinical and neuropathological features to HDLS (4). Based on their clinical and neuropathological similarities, HDLS and POLD have been proposed to belong to a single disease entity (2, 4, 16-18). Therefore, the molecular basis of HDLS and POLD has increasingly attracted much attention since the discovery of *CSF1R* as a causative gene for HDLS.

Our case suggests that the incidence of HDLS may be much higher than previously estimated because sporadic HDLS cases might be overlooked unless postmortem examinations are undertaken. We propose that more careful attention should be paid to HDLS as a possible cause of presenile dementia, regardless of a patient's family history. Now, a premortem diagnosis of HDLS can be established using a molecular analysis of *CSF1R*. Making an early diagnosis is of great importance in furthering the understanding of sequential changes in clinical and neuroradiological findings among patients with HDLS.

The authors state that they have no Conflict of Interest (COI).

Acknowledgement

We thank Ms. Eri Ishikawa and Kayo Suzuki (Research Center for Human and Environmental Sciences, Shinshu University) for their technical assistance in the molecular analysis of *CSF1R*.

This work was supported by Grants-in-Aid from the Research Committee for Hereditary Cerebral Small Vessel Disease and Associated Disorders, the Ministry of Health, Labour and Welfare of Japan.

References

1. Rademakers R, Baker M, Nicholson AM, et al. Mutations in the colony stimulating factor 1 receptor (*CSF1R*) gene cause hereditary diffuse leukoencephalopathy with spheroids. Nat Genet **44**: 200-205, 2012.
2. Marotti JD, Tobias S, Fratkin JD, Powers JM, Rohdes CH. Adult onset leukodystrophy with neuroaxonal spheroids and pigmented glia: report of a family, historical perspective, and review of the literature. Acta Neuropathol (Berl) **107**: 481-488, 2004.
3. Freeman SH, Hyman BT, Sims KB, et al. Adult onset leukodystrophy with neuroaxonal spheroids: clinical, neuroimaging and neuropathologic observations. Brain Pathol **19**: 39-47, 2009.
4. Wider C, Van Gerpen JA, DeArmond S, Shuster EA, Dickson DW, Wszolek ZK. Leukoencephalopathy with spheroids (HDLS) and pigmentary leukodystrophy (POLD): a single entity? Neurology **72**: 1953-1959, 2009.
5. van der Knaap MS, Naidu S, Kleinschmidt-Demasters BK, Kamphorst W, Weinstein HC. Autosomal dominant diffuse leukoencephalopathy with neuroaxonal spheroids. Neurology **54**: 463-468, 2000.
6. Yamashita M, Yamamoto T. Neuroaxonal leukoencephalopathy with axonal spheroids. Eur Neurol **48**: 20-25, 2002.
7. Moro-de-Casillas ML, Cohen ML, Riley DE. Leucoencephalopathy with neuroaxonal spheroids (LENAS) presenting as the cerebellar subtype of multiple system atrophy. J Neurol Neurosurg Psychiatry **75**: 1070-1072, 2004.
8. Keegan BM, Giannini C, Parisi JE, Lucchinetti CF, Boeve BF, Josephs KA. Sporadic adult-onset leukoencephalopathy with neuroaxonal spheroids mimicking cerebral MS. Neurology **70**: 1128-1133, 2008.
9. Kinoshita M, Yoshida K, Oyanagi K, Hashimoto T, Ikeda S. Hereditary diffuse leukoencephalopathy with axonal spheroids caused by R782H mutation in *CSF1R*: case report. J Neurol Sci **318**: 115-118, 2012.
10. Sundal C, Van Gerpen JA, Nicholson AM, et al. MRI characteristics and scoring in HDLS due to *CSF1R* gene mutations. Neurology **79**: 566-574, 2012.
11. Poll-The BT, Gärtner J. Clinical diagnosis, biochemical findings and MRI spectrum of peroxisomal disorders. Biochim Biophys Acta **1822**: 1421-1429, 2012.
12. Chabriat H, Bousser MG. Cerebral autosomal dominant arteriopathy with subcortical infarcts and leukoencephalopathy. In: Handbook of Clinical Neurology. Vol 89 (3rd series). Duyckaerts C, Litvan I, Eds. Elsevier, New York, 2008: 671-686.
13. Lyoo IK, Satlin A, Lee CK, Renshaw PF. Regional atrophy of the corpus callosum in subjects with Alzheimer's disease and multi-infarct dementia. Psychiatry Res **74**: 63-72, 1997.
14. Yamauchi H, Fukuyama H, Shio H. Corpus callosum atrophy in patients with leukoaraiosis may indicate global cognitive impairment. Stroke **31**: 1515-1520, 2000.
15. Yaldizli O, Atefy R, Gass A, et al. Corpus callousm index and long-term disability in multiple sclerosis patients. J Neurol **257**: 1256-1264, 2010.
16. Itoh K, Shiga K, Shimizu K, Muranishi M, Nakagawa M, Fushiki S. Autosomal dominant leukodystrophy with axonal spheroids and pigmented glia: clinical and neuropathological characteristics. Acta Neuropathol **111**: 39-45, 2006.
17. Ali ZS, Van Der Voorn JP, Powers JM. A comparative morphologic analysis of adult onset leukodystrophy with neuroaxonal spheroids and pigmented glia-a role for oxidative damage. J Neuropathol Exp Neurol **66**: 660-672, 2007.
18. Wong JC, Chow TW, Hazrati LN. Adult-onset leukoencephalopathy with axonal spheroids and pigmented glia can present as frontotemporal dementia syndrome. Dement Geriatr Cogn Disord **32**: 150-158, 2011.

INTERNAL MEDICINE

□ ORIGINAL ARTICLE □

Corpus Callosum Atrophy in Patients with Hereditary Diffuse Leukoencephalopathy with Neuroaxonal Spheroids: An MRI-based Study

Michiaki Kinoshita[1], Yasufumi Kondo[1], Kunihiro Yoshida[2], Kazuhiro Fukushima[1], Ken-ichi Hoshi[3], Keisuke Ishizawa[4], Nobuo Araki[4], Ikuru Yazawa[5], Yukihiko Washimi[6], Banyu Saitoh[7], Jun-ichi Kira[7] and Shu-ichi Ikeda[1]

Abstract

Objective Hereditary diffuse leukoencephalopathy with neuroaxonal spheroids (HDLS) is an adult-onset white matter disease that presents clinically with cognitive, mental and motor dysfunction. Several autopsy reports have indicated that the corpus callosum (CC), the largest bundle of white matter, is severely affected in patients with HDLS. The aim of this study was to evaluate corpus callosum atrophy (CCA) quantitatively in HDLS patients.

Methods We assessed CCA in six genetically-proven HDLS patients (HDLS group), in comparison with that observed in 20 patients with vascular dementia (VaD group) and 24 age-matched patients without organic central nervous system (CNS) disease (non-CNS group). Using midsagittal MR images, five measurements of the CC were obtained: the width of the rostrum (aa'), body (bb') and splenium (cc'), the anterior to posterior length (ab) and the maximum height (cd). Next, the corpus callosum index (CCI) was calculated as (aa' + bb' + cc')/ab.

Results All HDLS patients had white matter lesions in the CC and frontoparietal lobes on the initial MRI scans. Compared with that observed in the VaD and age-matched non-CNS groups, the CCI was significantly decreased in the HDLS group (with VaD group, $p<0.01$; with non-CNS group, $p<0.01$).

Conclusion This study showed significant atrophy of the CC in all HDLS patients on the initial MRI scans obtained 6-36 months after onset. We propose that the early appearance of CCA, frequently accompanied by high-intensity in the genu and/or splenium, on T2 images is an important diagnostic clue to HDLS.

Key words: hereditary diffuse leukoencephalopathy with neuroaxonal spheroids (HDLS), colony stimulating factor 1 receptor (CSF1R), white matter lesions (WMLs), corpus callosum atrophy (CCA), corpus callosum index (CCI)

(Intern Med 53: 21-27, 2014)
(DOI: 10.2169/internalmedicine.53.0863)

Introduction

Hereditary diffuse leukoencephalopathy with neuroaxonal spheroids (HDLS) is an adult-onset white matter disease caused by mutations in colony stimulating factor 1 receptor [*CSF1R* (1)]. HDLS is characterized clinically by cognitive, psychiatric and motor dysfunction that is frequently accom-

[1]Department of Medicine (Neurology and Rheumatology), Shinshu University School of Medicine, Japan, [2]Department of Brain Disease Research, Shinshu University School of Medicine, Japan, [3]Department of Neurology, Nagano Red-Cross Hospital, Japan, [4]Department of Neurology, Saitama Medical School, Japan, [5]Laboratory of Research Resources, Research Institute for Longevity Sciences, National Center for Geriatrics and Gerontology, Japan, [6]Department for Cognitive Disorders, National Center for Geriatrics and Gerontology, Japan and [7]Department of Neurology, Neurological Institute, Graduate School of Medical Sciences, Kyushu University, Japan
Received for publication April 26, 2013; Accepted for publication August 4, 2013
Correspondence to Dr. Kunihiro Yoshida, kyoshida@shinshu-u.ac.jp

Table 1. Clinical Characteristics of Six HDLS Patients

Patient	1	2	3	4	5	6
Sex	F	M	M	M	M	F
Age at disease onset (years)	51	41	53	40	55	27
Age at death (years)	alive	41	56	alive	62	alive
Family history	+	-	+	+	+	-
Neuropsychiatric symptoms						
Cognitive decline	+	+	+	+	+	+
Depression/Anxiety	-	+	+	+	+	?
Behavioral change	+	+	+	+	+	+
Frontal releasing signs	+	+	+	+	+	+
Pyramidal tract signs	+	-	+	-	+	+
Parkinsonism	+	+	+	+	+	?
Apraxia	-	+	+	+	?	+
Epilepsy	+	-	+	-	-	+
CSF1R mutation	R782H	K793T*	R777W	R777W	S759F	I794T*

*: genetically-determined sporadic case carrying a *de novo* mutation, ?: unknown or equivocal because of difficulty to evaluate symptoms

panied by epilepsy (2). The age of onset is quite variable, ranging from 8 to 78 years, and the mean duration of the illness has been reported to be 10 years (2) or 5.8 years (3). Due to its wide variety of neuropsychiatric symptoms and age of onset, HDLS mimics many neurological diseases, including vascular dementia (VaD), cerebral autosomal dominant arteriopathy with subcortical infarcts and leukoencephalopathy (CADASIL), frontotemporal dementia (FTD), multiple sclerosis (MS) and multisystem atrophy [MSA (4-7)].

MRI has significant value in evaluating the distribution and degree of white matter lesions (WMLs) and is indispensable for diagnosing HDLS. Recently, Sundal et al. reported the characteristics of 20 MRI scans of 15 patients with pathologically- and genetically-proven HDLS (3). They revealed that WMLs are predominantly frontal in patients with HDLS and that WMLs extending beyond the frontal lobes indicate rapid disease progression.

They also proposed a brain MRI scoring system for evaluating HDLS that appears to be very useful for tracking the natural history of HDLS and predicting the prognosis; however, this system places more emphasis on signal changes in the white matter (total WML score 42) than on atrophy (total atrophy score 13) (3).

Since the discovery of *CSF1R* as the causative gene, it has become possible to make a definitive diagnosis of HDLS in the early stage of the disease (1). We recently experienced a 41-year-old HDLS patient with the K793T mutation in *CSF1R* (patient 2, Table 1) (8). He was independent in daily life [modified Rankin Scale (mRS) 2] at the first presentation. His initial MRI scans (obtained six months after onset) showed minor WMLs within the frontoparietal lobes, corresponding to a total WMLs score of only 9/42 points on the MRI grading scale (3), however, diffuse atrophy of CC was already evident (8). This distinctive finding prompted us to assess early CC involvement in HDLS patients in greater detail.

Corpus callosum atrophy (CCA) has been noted in the postmortem examinations of advanced HDLS patients with diffuse widespread WMLs and severe brain atrophy (9-14).

Sundal et al. reported that CC involvement is frequently observed in HDLS patients on initial MRI scans, with the disease duration ranging from 0.5 to 5.0 years (3); however, in that study, CCA was roughly evaluated according to either its 'presence' or 'absence.' Therefore, in this study, we assessed MRI scans quantitatively to evaluate CCA in HDLS patients, especially in the early stage of disease without the presence of widespread WMLs on MRI.

Materials and Methods

Subjects

We examined 10 brain MRI scans of six HDLS patients (four men and two women; age at MRI scan: 29-57 years; mean age±standard deviation, 47.3±9.3 years) (Table 2). Mutations in *CSF1R* were identified in all patients. Three patients (patients 1, 3 and 4) had a family history consistent with autosomal inheritance (15), and two patients (patients 2 and 6) were confirmed to carry a *de novo CSF1R* mutation. One patient (patient 5) with a *CSF1R* mutation also had an affected brother; however, detailed information on their parents was not available. The detailed clinical information of the six HDLS patients is summarized in Table 1.

When enrolling patients with VaD, we adopted the guidelines of the National Institute for Neurological Disorders and Stroke-Association Internationale pour la Recherche et l'Enseignement en Neurosciences [NINDS-AIREN (16)]. We reviewed the medical records at our institution from April 2007 through March 2011. A diagnosis of VaD was made in patients fulfilling both the probable VaD criteria in the NINDS-AIREN and the following additional requirements: 1) an age under 80 years, 2) no family history of neurological or psychiatric diseases, 3) midsagittal MR images available for measurement. We ultimately identified 20 consecutive patients with VaD (11 men and nine women; age at MRI scan: 42-79 years, mean 68.5±7.9 years). The degree of clinical disability at the time of the MRI scan was assessed in the HDLS and VaD groups using the mRS defined by Sulter et al. (17).

The age-matched control group without organic central

Table 2. Summary of the MRI Findings

HDLS (n = 6)	Age at	Age at	Disease	mRS#	HDLS MRI severity score*			Corpus callosum atrophy								Evans
Patient	onset (years)	MRI (years)	duraation until the MRI scan (months)		Total WML score (corpus callosum)	Total atrophy score (corpus callosum)	Total score	ab (L)	aa'	bb'	cc' (B: body)	cd (H: height)	CCI	B/H	B/L	index
1 (1)	51	52	19	2	12 (5)	4 (1)	16	61.0	5.39	5.71	2.53	28.14	0.224	0.090	0.042	0.293
1 (2)		57	72	5	23 (6)	10 (1)	33	64.7	2.62	3.85	2.02	34.90	0.131	0.057	0.031	0.371
2 (1)	41	41	6	2	5 (1)	4 (1)	9	72.9	5.10	6.37	2.95	30.56	0.198	0.097	0.040	0.330
2 (2)		41	11	3	9 (3)	4 (1)	13	73.9	3.72	4.40	2.73	31.33	0.147	0.087	0.037	0.344
3 (1)	53	56	36	3	12 (5)	5 (1)	17	69.0	6.07	6.05	4.18	30.27	0.236	0.138	0.061	0.290
3 (2)		57	48	5	16 (6)	9 (1)	25	NA	NA	NA	NA	NA	NA	NA	NA	0.320
4 (1)	40	41	14	2	15 (6)	9 (1)	24	78.3	8.91	6.08	2.32	34.30	0.221	0.068	0.030	0.360
4 (2)		42	28	3	16 (6)	9 (1)	25	79.1	9.64	4.45	3.13	36.15	0.218	0.087	0.040	0.371
5	55	57	33	4	21 (6)	8 (1)	32	NA	NA	NA	NA	NA	NA	NA	NA	NA
6	27	29	8	4	17 (4)	4 (1)	22	60.7	6.73	9.37	2.33	19.83	0.304	0.119	0.038	0.286
average	44.500	47.300	27.500	3.300			21.600	69.954	6.023	5.785	2.775	30.685	0.210	0.093	0.040	0.331
SD	9.691	9.285	19.679	1.100			7.432	6.818	2.237	1.612	0.628	4.815	0.050	0.024	0.009	0.034
VaD (n = 20)																
average		68.500		2.750				72.620	8.160	7.992	4.689	28.479	0.289	0.169	0.065	0.272
SD		7.940		0.887				5.484	1.566	1.540	0.750	4.151	0.050	0.039	0.011	0.026
non-CNS (n = 24)																
average		49.917						71.141	10.157	10.609	5.635	27.221	0.371	0.208	0.079	0.246
SD		13.789						4.253	2.076	1.808	1.054	2.789	0.056	0.039	0.014	0.022

NA: not analyzed, #: modified Rankin Scale (17), *: proposed by Sundal et al. (3)

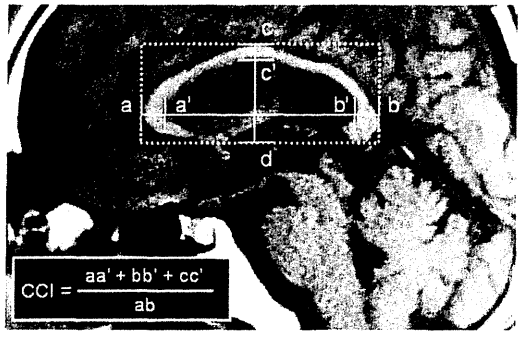

Figure 1. Determination of the corpus callosum index (CCI) using a midsagittal slice on a T1-weighted MR image (HDLS patient 2 in Table 1, 41-year-old man).

nervous system diseases (non-CNS group) included 24 patients (15 men and nine women; age at MRI scan: 29-73 years, mean 49.9±13.8 years). Their diagnoses were as follows: myasthenia gravis (n=6), psychosomatic disorder (n=5), benign paroxysmal positional vertigo (n=3), Guillain-Barré syndrome or Fisher syndrome (n=3), spinal canal stenosis (n=2), spinal cord tumor (n=2; able to exclude multiple sclerosis), brachial plexus neuropathy or neuralgic amyotrophy (n=2) and facioscapulohumeral muscular atrophy (FSH) (n=1). Brain MRI was conducted to rule out intracranial lesions in these patients. None of the patients had WMLs on MRI, except for a small amount of lacunar infarctions.

MRI assessments

The brain MRI scans of the VaD group and non-CNS group were performed in our hospital with a 1.5 Tesla Magnetom Avanto scanner (Siemens AG, Erlangen, Germany). T1-weighted images were obtained using a spin-echo technique (TE=12-26 ms, TR=250-500 ms, slice thickness=3-4 mm). The scans of the HDLS patients were performed in four different hospitals, patients 1-4 being examined using the same scanner as at our hospital (1.5 Tesla Magnetom Avanto, using the same acquisition protocol as the other groups). All of the MRI scans were measured independently once each by one of the authors (YK) and two additional examiners (YT and KT) who were blind to the clinical information, including the diagnoses and ages of the patients. All measurements were obtained using a computerized measurement tool on screen on a picture archiving and communication system (PACS) workstation. We measured the corpus callosum using midsagittal T1-weighted images according to previous reports (18-20). Five measurements of the CC were obtained (Fig. 1): the width of the rostrum (aa'), body (cc', abbreviated as B) and splenium (bb'), the anterior to posterior length (ab, abbreviated as L) and the maximum height (cd, abbreviated as H). The corpus callosum index (CCI), which has been reported to be a marker for brain atrophy in MS patients (18, 19), was calculated as (aa'+bb'+cc')/ab. The ratios B/L and B/H were also calculated. The Evans index (the maximum distance between the two anterior horns/the maximum transverse inner diameter of the skull at the same level) was measured using axial T1-weighted images. A comparison between the three investigators' evaluations of each indicator of the CCA and the Evans index was made with the intraclass correlation coefficiency (*ICC*) and internal consistency using Cronbach's alpha coefficient. In addition, we assessed the severity of WMLs and brain atrophy according to the MRI grading system proposed by Sundal et al. (3).

Statistical analysis

The statistical analysis was carried out using the nonparametric Mann-Whitney U-test to compare the indicators of CCA (aa', bb', cc' (B), ab (L), cd (H), BL, BH and CCI) and the Evans index between the HDLS group and each control group. We considered p values of <0.05 or less to be statistically significant.

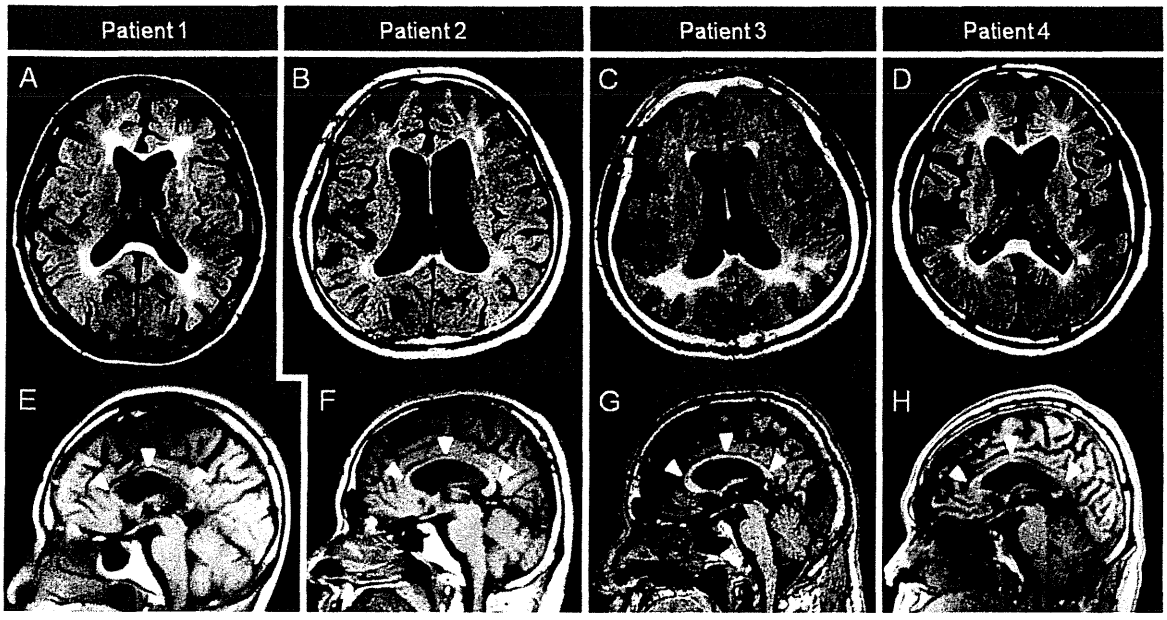

Figure 2. Representative MRI findings of four HDLS patients. A-D: Axial FLAIR images showing patchy or confluent periventricular-dominant white matter lesions and hyperintensity signals in the CC, especially in the splenium. E-H: Midsagittal T1-weighted images showing severe diffuse CC atrophy (arrowheads). (A and E: Patient 1 at age 52 (approximately 19 months after onset); B and F: Patient 2 at age 41 (approximately 11 months after onset); C and G: Patient 3 at age 56 (approximately three years after onset); D and H: Patient 4 at age 42 (approximately 14 months after onset), each patient number corresponding to that in Tables 1 and 2).

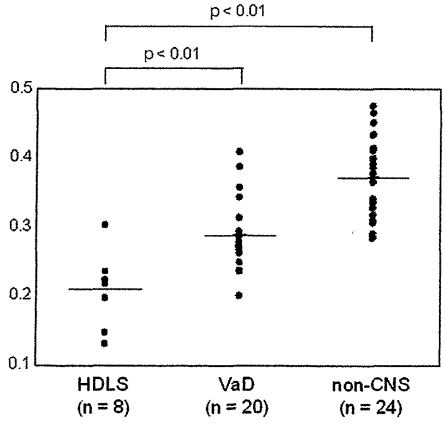

Figure 3. Distribution of the corpus callosum index (CCI) in the patients with HDLS, vascular dementia (VaD) and control individuals without organic central nervous system diseases (non-CNS). The CCI was significantly decreased in the HDLS group (0.210±0.050) compared with that observed in the VaD group (0.289±0.050) ($p<0.01$) and age-matched non-CNS group (0.371±0.056) ($p<0.01$). The horizontal bar indicates the mean of each group.

Results

All patients with HDLS had WMLs in the CC and fronto-parietal lobes (Fig. 2; Table 2). The WMLs extended to the temporal lobes in three patients. The total MRI severity scale for HDLS (3) ranged from 9 to 33 (Table 2). As the disease progressed, volume loss of the cerebral white matter became evident. None of the patients had high-intensity signals in the temporal tips or external capsules. Four patients (seven scans) were screened for cerebral microbleeds using T2*-weighted images; however, no such bleeding was detected, whereas 11 of the 12 patients (91.7%) examined in the VaD group had cerebral microbleeds.

Hyperintense signals and atrophy in the CC were detected on all 10 MRI scans in the six patients (Fig. 2; Table 2). The CCI was significantly decreased in the HDLS group (0.210±0.050) compared with that observed in the VaD group (0.289±0.050) ($p<0.01$) and age-matched non-CNS group (0.371±0.056) ($p<0.01$) (Fig. 3; Table 2). The B/H index (cc'/cd in Fig. 1) was also significantly reduced in the HDLS group (0.093±0.024) compared to that observed in the VaD group (0.169±0.039) ($p<0.01$) and non-CNS group (0.208±0.039) ($p<0.01$). Similarly, the B/L index (cc'/ab in Fig. 1) was significantly reduced in the HDLS group (0.040±0.009) compared to that observed in the VaD group (0.065±0.011) ($p<0.01$) and age-matched non-CNS group (0.079±0.014) ($p<0.01$). The Evans index, an indicator of lateral ventricle dilatation, was significantly larger in the HDLS group (0.331±0.034) than in the VaD group (0.272±0.026) ($p<0.01$) or non-CNS group (0.246±0.022) ($p<0.01$). The inter-rater reliability and internal consistency of the total measurements were almost good (*ICC*=0.755-0.951; Cronbach's alpha=0.907-0.986) (Table 3).

Table 3. Inter-rater Reliability and Internal Consistency of the Indicators of Corpus Callosum Atrophy and the Evans Index

	HDLS group (n = 8)		VaD group (n = 20)		Non-CNS control group (n=24)		Total (n = 52)	
Items	*ICC*	Cronbach's alpha	*ICC*	Cronbach's alpha	*ICC*	Cronbach's alpha	*ICC*	Cronbach's alpha
ab (L: length)	0.992	0.999	0.949	0.987	0.920	0.976	0.951	0.986
aa'	0.899	0.962	0.575	0.840	0.615	0.823	0.755	0.907
bb'	0.820	0.940	0.627	0.840	0.585	0.840	0.792	0.927
cc' (B: body)	0.656	0.883	0.577	0.801	0.736	0.895	0.832	0.940
cd (H: Height)	0.855	0.943	0.892	0.977	0.815	0.953	0.867	0.963
B/H	0.688	0.916	0.724	0.895	0.692	0.889	0.933	0.979
B/L	0.615	0.864	0.598	0.815	0.737	0.895	0.842	0.950
CCI	0.840	0.946	0.738	0.904	0.565	0.876	0.830	0.938
Evans index	0.913	0.970	0.844	0.950	0.853	0.960	0.859	0.952

ICC: Intraclass correlation coefficiency

Discussion

The occurrence of CCA with WMLs has been reported in some demential disorders, such as VaD, including Binswanger's disease, and CADASIL, MS and leukodystrophies, including HDLS. This was a quantitative study conducted to understand CC involvement in HDLS itself, and the aim was not primarily to compare the disease with the occurrence of CCA in VaD for diagnostic purposes to distinguish it from HDLS. We selected a VaD group as a control simply because VaD is the most common and representative disease involving CCA with WMLs.

Due to their clinical and neuroradiological similarities, it is sometimes difficult to differentiate between HDLS and other diseases involving CCA with WMLs, especially in the early stage of the disease. The lack of a family history does not preclude the possibility of HDLS, as several sporadic patients who fulfill the clinical and neuropathological criteria for HDLS have been reported (4, 5, 8, 21). Furthermore, the occurrence of HDLS due to a *de novo CSF1R* mutation has hitherto been confirmed in two families in which the parents of the patient had no mutations of interest (1, 8), and one such family was newly added in this study (patient 6). The most reliable method of discriminating HDLS is currently genetic testing for *CSF1R*. Because genetic testing for *CSF1R* is not presently commercially available, identifying laboratory or neuroradiological hallmarks of HDLS is of value in order to select candidates for further processing to genetic testing.

Recently, Sundal et al. reported that 14 of 15 patients exhibited CC involvement (the disease duration at the initial MRI study ranged from 0.5 to 5.0 years). The CC involvement included atrophy (eight patients), T2 and FLAIR high signal intensity (11 patients) and both atrophy and signal changes in the CC (five patients) (3). These data appear to indicate that hyperintense signals and atrophy in the CC are not correlated with each other. This may be partly because CCA was evaluated using a score of 0 (absence of atrophy) or 1 (presence of atrophy). Therefore, we evaluated CCA quantitatively in this study.

As to data regarding the measurement of CC in healthy Japanese subjects, Takeda et al. reported CC measurements in 205 Japanese individuals without CNS disorders (94 men, mean age: 57.3±20.8 years; range: 6-90 years; and 111 women, 61.2±17.6 years; range: 9-86 years). These values are similar to those of our study, including the widths of the rostrum (aa'): mean ± SD 9.91±1.82 (our non-CNS group, 10.16±2.08), body (bb'): 5.58±1.08 (5.64±1.05), splenium (cc'): 9.94±1.56 (10.61±1.81) and anterior to posterior length (ab): 69.7±4.24 (71.14±4.24), although there was a difference in the range of ages between the two studies. In another study, the CC measurements of 15 Japanese healthy men (mean age: 56.2±6.9) were reported as follows: aa': 10.6±1.4, bb': 5.3±1.1, cc': 10.4±1.4 and ab: 72.7±8.5 (22). These data were also very close to those of our measurements, as well as the ranges of ages, in the non-CNS group. In addition, the CCI was 0.362 when calculated using the mean data for the trial (our non-CNS group: 0.371±0.056). These results support the reliability of the CCI data for our non-CNS group, in spite of the limitation in the number of cases.

In our study, all of the patients had abnormal hyperintensive signals in the CC on their initial MRI scans (disease duration ranging from six to 36 months). Furthermore, the CCI was significantly decreased when compared with that observed in the VaD and age-matched non-CNS groups. In this study, the mean age at MRI in the VaD group (68.5 years) was much higher than that noted in the HDLS group (47.3 years). Takeda et al. showed that the widths of the rostrum (aa'), body (cc', B) and splenium (bb') of the CC decrease with age in normal Japanese individuals (20). Conversely, the maximum height (cd, H) and anterior to posterior length (ab, L) gradually increase with age. These data indicate that the CCI, B/H and B/L decrease with age. Taking the difference in the mean age between the HDLS and VaD groups into consideration, we can say that the decreases in the CCI, B/H and B/L in the HDLS group were conspicuous compared with those observed in the VaD group.

In addition, the CCI observed in the HDLS patients was much less than that at diagnosis in the MS patients (0.345±

0.04; mean age 42±11 years, n=169) reported by Yaldizli et al. (19). Therefore, we think that CCA should be monitored more carefully in HDLS patients.

The LADIS study indicated that CCA is associated with cognitive decline that coexists independently with white matter hyperintensity and stroke (23, 24). In particular, overall CCA is correlated with the slowing of processing or mental speed (23, 24). In patients with HDLS, frontal lobe signs and symptoms are frequently observed in the early stage of the disease. This is consistent with the observation of Sundal et al. that WMLs are predominantly frontal (3), as supported by the findings of this study. Additionally, it is possible that the early involvement of the CC contributes to the psychomotor dysfunction observed in HDLS patients.

CCA is observed in elderly persons, as well as in patients with cerebrovascular and neurodegenerative diseases (25-31). Several underlying mechanisms for CCA have been postulated (25-30). In Alzheimer's disease patients, CCA primarily reflects the loss of the corresponding cortical neurons (Wallerian degeneration hypothesis) (26, 28, 29) and/or age-related myelin breakdown (retrogenesis hypothesis) (28, 29, 32). Conversely, in patients with cerebrovascular diseases, CCA is closely related to cerebral WMLs (26, 27, 31), assuming that ischemic damage causes focal edema and inflammation with subsequent axonal disruption (26). The mechanism underlying the development of CCA in patients with HDLS is likely to be different from that observed in those with Alzheimer's disease or cerebrovascular disease because CCA develops in the earlier stage of the disease and progresses more rapidly in HDLS.

HDLS is neuropathologically characterized by the extensive loss of myelin sheaths, axonal destruction and the presence of numerous axonal spheroids, pigmented macrophages and astrogliosis (2, 9-14). These changes were clearly observed in the centrum semiovale of the cerebral white matter in one of our patients (patient 2) (8). That patient died of sepsis caused by severe intestinal infection at age 41 in the early stage of the disease (mRS3). Macroscopically, the CC was diffusely thin (data not shown). Histologically, the localized portion of the splenium of the CC that exhibited T2 and FLAIR high signals on MRI demonstrated a severe loss of myelin and axons with axonal spheroids, as seen in the centrum semiovale. This is a primary pathological process of axonal disruption in HDLS. On the other hand, the basic structure was relatively preserved in the other parts of the CC, where the number of axons was decreased; however, the findings of tissue destruction, including localized myelin loss, disarrangement of axons and the presence of spheroids and activated macrophages, were quite mild. This likely reflects a secondary change due to axonal damage in the proximal parts of the commissural fibers. CC involvement in HDLS patients is therefore considered to be caused by these combined pathological processes. Additionally, ischemic changes, including small infarcts and microvascular fibrohyalinosis, were almost absent in the entire CC; therefore, the pathologic mechanism appears to be basically different between HDLS and cerebrovascular disease.

The present study is associated with several limitations. First, the number of HDLS patients was very small. The incidence of HDLS in the Japanese population remains unknown because genetic testing for *CSF1R* has only recently been introduced into clinical practice, and genetically-proven cases are very small in number at present. Second, the patients in the VaD group in this study were rather heterogeneous because this was a retrospective study. The mRS of the VaD group (2.75±0.89) was not significantly different from that of the HDLS group (3.30±1.10); however, the cognitive function levels varied from subnormal to severe dementia in the VaD group. As judged according to the mRS, cognitive, mental and motor dysfunction was variable in both the HDLS and VaD groups; therefore, it was not possible to make MRI comparisons between these two groups after adjusting for the clinical status. Third, there was overlap in the values of the CCI between the HDLS and VaD patients; therefore, we were unable to present any diagnostic cutoff values for distinguishing HDLS from VaD.

In conclusion, despite the several limitations described above, our quantitative neuroimaging study clearly showed the presence of CCA on the initial MRI scans (6-36 months after disease onset) in HDLS patients. Our findings suggest that the presence of CCA on MRI frequently accompanied by high intensity in the genu and/or splenium on T2 and FLAIR images is a useful finding indicative of HDLS.

The authors state that they have no Conflict of Interest (COI).

Acknowledgement

We thank the two examiners (Mr. Yusuke Takahashi and Mr. Kazuhito Takahashi) for their assistance in measuring the MR images. This work was supported by Grants-in-Aid from the Research Committee for hereditary cerebral small vessel disease and associated disorders of the Ministry of Health, Labour and Welfare of Japan (Dr. Kunihiro Yoshida).

References

1. Rademakers R, Baker M, Nicholson AM, et al. Mutations in the colony stimulating factor 1 receptor (*CSF1R*) gene cause hereditary diffuse leukoencephalopathy with spheroids. Nat Genet **44**: 200-205, 2012.
2. Wider C, Van Gerpen JA, DeArmond S, Shuster EA, Dickson DW, Wszolek ZK. Leukoencephalopathy with spheroids (HDLS) and pigmentary leukodystrophy (POLD). A single entity? Neurology **72**: 1953-1959, 2009.
3. Sundal C, Van Gerpen JA, Nicholson AM, et al. MRI characteristics and scoring in HDLS due to *CSF1R* gene mutations. Neurology **79**: 566-574, 2012.
4. Moro-de-Casillas ML, Cohen ML, Riley DE. Leucoencephalopathy with neuroaxonal spheroids (LENAS) presenting as the cerebellar subtype of multiple system atrophy. J Neurol Neurosurg Psychiatry **75**: 1070-1072, 2004.
5. Keegan BM, Giannini C, Parisi JE, Lucchinetti CF, Boeve BF, Josephs KA. Sporadic adult-onset leukoencephalopathy with neuroaxonal spheroids mimicking cerebral MS. Neurology **70**: 1128-1133, 2008.
6. Wong JC, Chow TW, Hazrati L-N. Adult-onset leukoencephalopa-

thy with axonal spheroids and pigmented glia can present as frontotemporal dementia syndrome. Dement Geriatr Cogn Disord **32**: 150-158, 2011.

7. Sundal C, Lash J, Aasly J, et al. Hereditary diffuse leukoencephalopathy with axonal spheroids (HDLS): A misdiagnosed disease entity. J Neurol Sci **314**: 130-137, 2012.
8. Kondo Y, Kinoshita M, Fukushima K, Yoshida K, Ikeda S. Early involvement of the corpus callosum in a patient with hereditary diffuse leukoencephalopathy with spheroids carrying the *de novo* K793T mutation of *CSF1R*. Intern Med **52**: 503-506, 2013.
9. van der Knaap MS, Naidu S, Kleinschmidt-Demasters BK, Kamphorst W, Weinstein HC. Autosomal dominant diffuse leukoencephalopathy with neuroaxonal spheroids. Neurology **54**: 463-468, 2000.
10. Terada H, Ishizu H, Yokota O, et al. An autopsy case of hereditary diffuse leukoencephalopathy with spheroids, clinically suspected of Alzheimer's disease. Acta Neuropathol **108**: 538-545, 2004.
11. Marotti JD, Tobias S, Fratkin JD, Powers JM, Rohdes CH. Adult onset leukodystrophy with neuroaxonal spheroids and pigmented glia: report of a family, historical perspective, and review of the literature. Acta Neuropathol **107**: 481-488, 2004.
12. Itoh K, Shiga K, Shimizu K, Muranishi M, Nakagawa M, Fushiki S. Autosomal dominant leukodystrophy with axonal spheroids and pigmented glia: clinical and neuropathological characteristics. Acta Neuropathol **111**: 39-45, 2006.
13. Baba Y, Ghetti B, Baker MC, et al. Hereditary diffuse leukoencephalopathy with spheroids: clinical, pathologic and genetic studies of a new kindred. Acta Neuropathol **111**: 300-311, 2006.
14. Freeman SH, Hyman BT, Sims KB, Hedley-Whyte ET, Vossough A, Frosch MP. Adult onset leukodystrophy with neuroaxonal spheroids: clinical, neuroimaging and neuropathologic observations. Brain Pathol **19**: 39-47, 2009.
15. Kinoshita M, Yoshida K, Oyanagi K, Hashimoto T, Ikeda S. Hereditary diffuse leukoencephalopathy with axonal spheroids caused by R782H mutation in *CSF1R*: case report. J Neurol Sci **318**: 115-118, 2012.
16. Román GC, Tatemichi TK, Erkinjuntti T, et al. Vascular dementia: diagnostic criteria for research studies. Report of the NINDS-AIREN International Workshop. Neurology **43**: 250-260, 1993.
17. Sulter G, Steen C, De Keyser J. Use of the Barthel index and modified Rankin scale in acute stroke trial. Stroke **30**: 1538-1541, 1999.
18. Figueira FFA, dos Santos VS, Figueira GMA, da Silva ÂCM. Corpus callosum index: a practical method for lomg-term follow-up in multiple sclerosis. Arq Neuropsiquiatr **65**: 931-935, 2007.
19. Yaldizli O, Atefy R, Gass A, et al. Corpus callousm index and long-term disability in multiple sclerosis patients. J Neurol **257**: 1256-1264, 2010.
20. Takeda S, Hirashima Y, Ikeda H, Yamamoto H, Sugino M, Endo S. Determination of indices of the corpus callosum associated with normal aging in Japanese individuals. Neuroradiol **45**: 513-518, 2003.
21. Yamashita M, Yamamoto T. Neuroaxonal leukoencephalopathy with axonal spheroids. Eur Neurol **48**: 20-25, 2002.
22. Oishi M, Mochizuki Y, Shikata E. Corpus callosum atrophy and cerebral blood flow in chronic alcoholics. J Neurol Sci **162**: 51-55, 1999.
23. Jokinen H, Ryberg C, Kalska H, et al; LADIS group. Corpus callosum atrophy is associated with mental slowing and executive deficits in subjects with age-related white matter hyperintensities: the LADIS study. J Neurol Neurosurg Psychiatr **78**: 491-496, 2007.
24. Jokinen H, Frederiksen KS, Garde E, et al. Callosal tissue loss parallels subtle decline in psychomotor speed. a longitudinal quantitative MRI study. The LADIS Study. Neuropsychologia **50**: 1650-1655, 2012.
25. Meguro K, Constans JM, Courtheoux P, Theron J, Viader F, Yamadori A. Atrophy of the corpus callosum correlates with white matter lesions in patients with cerebral ischaemia. Neuroradiology **42**: 413-419, 2000.
26. Tomimoto H, Lin JX, Matsuo A, et al. Different mechanisms of corpus callosum atrophy in Alzheimer's disease and vascular dementia. J Neurol **251**: 398-406, 2004.
27. Ryberg C, Rostrup E, Sjöstrand K, et al; LADIS study group. White matter changes contribute to corpus callosum atrophy in the elderly: the LADIS study. AJNR Am J Neuroradiol **29**: 1498-1504, 2008.
28. Di Paola M, Di Iulio F, Cherubini A, et al. When, where, and how the corpus callosum changes in MCI and AD: a multimodel MRI study. Neurology **74**: 1136-1142, 2010.
29. Di Paola M, Luders E, Di Iulio F, et al. Callosal atrophy in mild cognitive impairment and Alzheimer's disease: different effects in different stages. Neuroimage **49**: 141-149, 2010.
30. Frederiksen KS, Garde E, Skimminge A, et al. Corpus callosum tissue loss and development of motor and global cognitive impairment: the LADIS study. Dement Geriatr Cogn Disord **32**: 279-286, 2011.
31. Lee DY, Fletcher E, Martinez O, et al. Vascular and degenerative processes differentially affect regional interhemispheric connections in normal aging, mild cognitive impairment, and Alzheimer disease. Stroke **41**: 1791-1797, 2010.
32. Bartzokis G. Age-related myelin breakdown: a development model of cognitive decline and Alzheimer's disease. Neurobiol Aging **25**: 5-18, 2004.

Neuroradiology
DOI 10.1007/s00234-012-1105-x

DIAGNOSTIC NEURORADIOLOGY

Detection of early neuronal damage in CADASIL patients by q-space MR imaging

Kei Yamada · Koji Sakai · Kentaro Akazawa · Naozo Sugimoto · Masanori Nakagawa · Toshiki Mizuno

Received: 25 July 2012 / Accepted: 5 October 2012

Abstract
Introduction q-Space imaging is a novel magnetic resonance (MR) technique that enables the assessment of ultrastructural changes of white matter. We hypothesized that this technique would facilitate the assessment of the progressive nature of neuronal damage seen in cerebral autosomal dominant arteriopathy with subcortical infarcts and leukoencephalopathy (CADASIL).
Methods This study was approved by the institutional review board. Seven consecutive adult patients (five men and two women) with the CADASIL gene mutation were studied. Two patients were preclinical cases without overt episodes of stroke. The control group consisted of five normal volunteers. All MR examinations were performed using a 1.5-T whole-body imager. q-Space imaging was performed using a single-shot, echo-planar imaging technique and $\Delta/\delta = 142/17$ ms. Gradient magnitudes were increased in nine steps to reach a maximal b value of 10,000 s/mm^2. Total acquisition time of q-space imaging was 25 min. The ADC maps calculated from the $b = 1{,}000$ images were used for comparisons.
Results Both q-space imaging and ADC maps depicted progressive neuronal damage. Early neuronal damage was especially well depicted using q-space imaging, with preferential involvement of the frontal lobes and central gray matters. Later progression was better depicted by $b = 1{,}000$ ADC maps at the temporal lobes. Visual assessment of images revealed a trend for occipital lobe sparing, especially on q-space imaging.
Conclusion q-Space imaging demonstrated early neuronal damage in a characteristic distribution. Since this method appears to be sensitive to early neuronal damage, it could conceivably aid in monitoring patients in the preclinical stage and may help in assessing the effects of future medical interventions.

Keywords CADASIL · White matter · Diffusion-weighted imaging · q-Space imaging · Mean displacement (MD)

Abbreviations

CC	Corpus callosum
CGM	Central gray matters
MD	Mean displacement
SPG	Short pulse gradient

Introduction

Cerebral autosomal dominant arteriopathy with subcortical infarcts and leukoencephalopathy (CADASIL) is a hereditary condition causing recurrent subcortical strokes. It is caused by mutations in the notch3 gene. Recurrent vascular events, headache, mood disorders, and progressive cognitive decline are the main clinical manifestations. Histopathological studies have indicated that the characteristic features are arteriopathy of small- and middle-sized arteries without atherosclerosis or amyloid deposition. This arteriopathy results in an "earthen pipe state," by which cerebral autoregulation is lost [1]. This

K. Yamada (✉) · K. Akazawa
Department of Radiology, Graduate School of Medical Science,
Kyoto Prefectural University of Medicine,
Kajii-cho, Kawaramachi Hirokoji Sagaru, Kamigyo-ku,
Kyoto City, Kyoto 602-8566, Japan
e-mail: kyamada@koto.kpu-m.ac.jp

M. Nakagawa · T. Mizuno
Department of Neurology, Graduate School of Medical Science,
Kyoto Prefectural University of Medicine,
Kajii-cho, Kawaramachi Hirokoji Sagaru, Kamigyo-ku,
Kyoto City, Kyoto 602-8566, Japan

K. Sakai · N. Sugimoto
Department of Human Health Science,
Graduate School of Medicine, Kyoto University,
53 Shogoin Kawara-cho, Sakyo-ku,
Kyoto City, Kyoto 606-8507, Japan

Published online: 25 October 2012

leads to ischemia, demyelination, and reactive gliosis, with relative sparing of the subcortical U-fibers [1].

Neuroimaging shows both focal lacunar infarcts and diffuse white matter ischemic changes. Magnetic resonance (MR) imaging is especially useful and plays an important initial role in the diagnosis, since studies have demonstrated characteristic features, such as involvement of the anterior temporal pole and external capsule [2].

Another potential role of imaging is to monitor disease progression. However, the progression of white matter damage on fluid attenuated inversion recovery (FLAIR) images typically levels off at the fifth decade, when hyperintense lesions become widespread throughout the cerebral white matter [3]. Furthermore, there is no established neuroimaging technique that enables monitoring of patients in the preclinical stage. Thus, an imaging method that would enable better characterization of the brain at the earliest stage would be of clinical benefit.

Assessment of the disease status of CADASIL patients has been attempted by the use of diffusion-weighted imaging (DWI) and diffusion tensor imaging (DTI) techniques [4]. These depict tissue damage through ADC measurements even in areas that appear normal on conventional MR [5]. Furthermore, the DTI histogram metrics have been shown to be more sensitive than conventional imaging studies in predicting disease progression [4].

Recent studies have further extended the conventional DTI technique to use much higher b values (e.g., 10,000 s/mm^2) [6–9]. The method is known as q-space imaging; it was originally designed to measure the compartment size of porous material filled with water [6]. Owing to various technical challenges, it was initially limited to study animals [10–13], but was later extended to clinical imaging [14–17]. This technique with high b values enables measurement of the mean displacement (MD) of the most slowly diffusing water molecules. By applying this technique to the central nervous system, one can now perform ultrastructural assessment of the compartment size of white matter [10, 11, 14, 18]. For instance, excellent agreements have been found between axonal size as obtained on q-space imaging and histology of optic nerves and the spinal cord [19, 20].

The aim of this study was to test the feasibility of this novel technique to assess the neuronal damage in CADASIL patients. More specifically, whether one could better observe the progressive nature of neuronal damage in CADASIL patients was examined.

Methods

Patient population

This study was approved by the institutional review board. Seven consecutive adult patients (five men and two women) ranging in age from 44 to 76 (mean, 55) years were studied. All of these patients were genetically proven to have CADASIL through direct sequencing (i.e., NOTCH3 mutations including C106R, R141C, or R332C). All of them had cerebral white matter lesions on FLAIR to various extents. The study period was from August 2010 to April 2011. The control group consisted of five subjects (mean age, 41 years; four men and one woman) who volunteered. None of them had a history of neurological disease or head trauma. All were in excellent health, and they did not exhibit any white matter lesions on MR.

Data acquisition

All MR examinations were performed using a 1.5-T whole-body imager (Philips Medical Systems, Best, the Netherlands). In all MRI scans, the field of view was 23 cm. DWI for q-space imaging was acquired using a single-shot, echo-planar imaging technique [repetition time (TR)/echo time

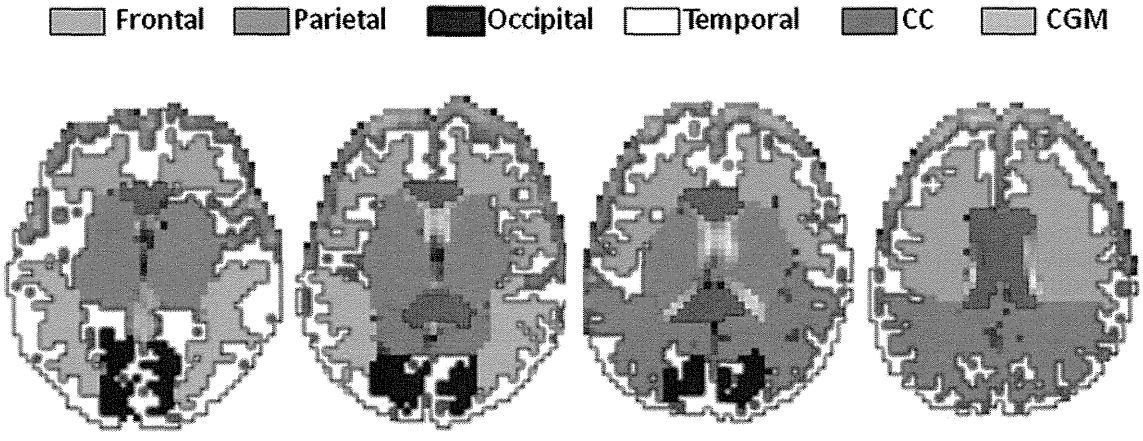

Fig. 1 Template for ROI analysis. Manual segmentation of the white matter of four lobes, corpus callosum, and CGM was performed as indicated in this figure

(TE)=6,000/173 ms], Δ/δ=142/17 ms (effective diffusion time (T_{diff})=136 ms) and a matrix of 128×128, without cardiac gating. Gradient magnitudes were increased in nine steps to reach a maximal b value of 10,000 s/mm^2 and a maximal q value of 855 cm^{-1}. The b values used were 0, 10, 60, 100, 300, 600, 1,000, 3,000, 6,000, and 10,000 s/mm^2. Motion-sensitizing gradients were applied in 15 directions. A total of twelve 3-mm-thick sections were obtained without intersection gaps to cover the central parts of the brain, including the basal ganglia and the upper limit of the corpus callosum. These diffusion-weighted images were motion/distortion corrected to match the b=0 images on the console of the MR unit. The q-space data set included 136 images per slice (nine diffusion images in 15 diffusion gradient directions) with total acquisition time of 25 min.

Data postprocessing

Data were sent to an offline computer for further analysis on a homemade software. The q-space analysis was performed on a pixel-by-pixel basis, as previously described [14]. High b value components above 10,000 s/mm^2 were zero-filled upon the analysis. First, the mean displacement distribution profile was calculated for each gradient direction by Fourier transformation of the signal decay. The full width at half maximum of the displacement distribution profile was then

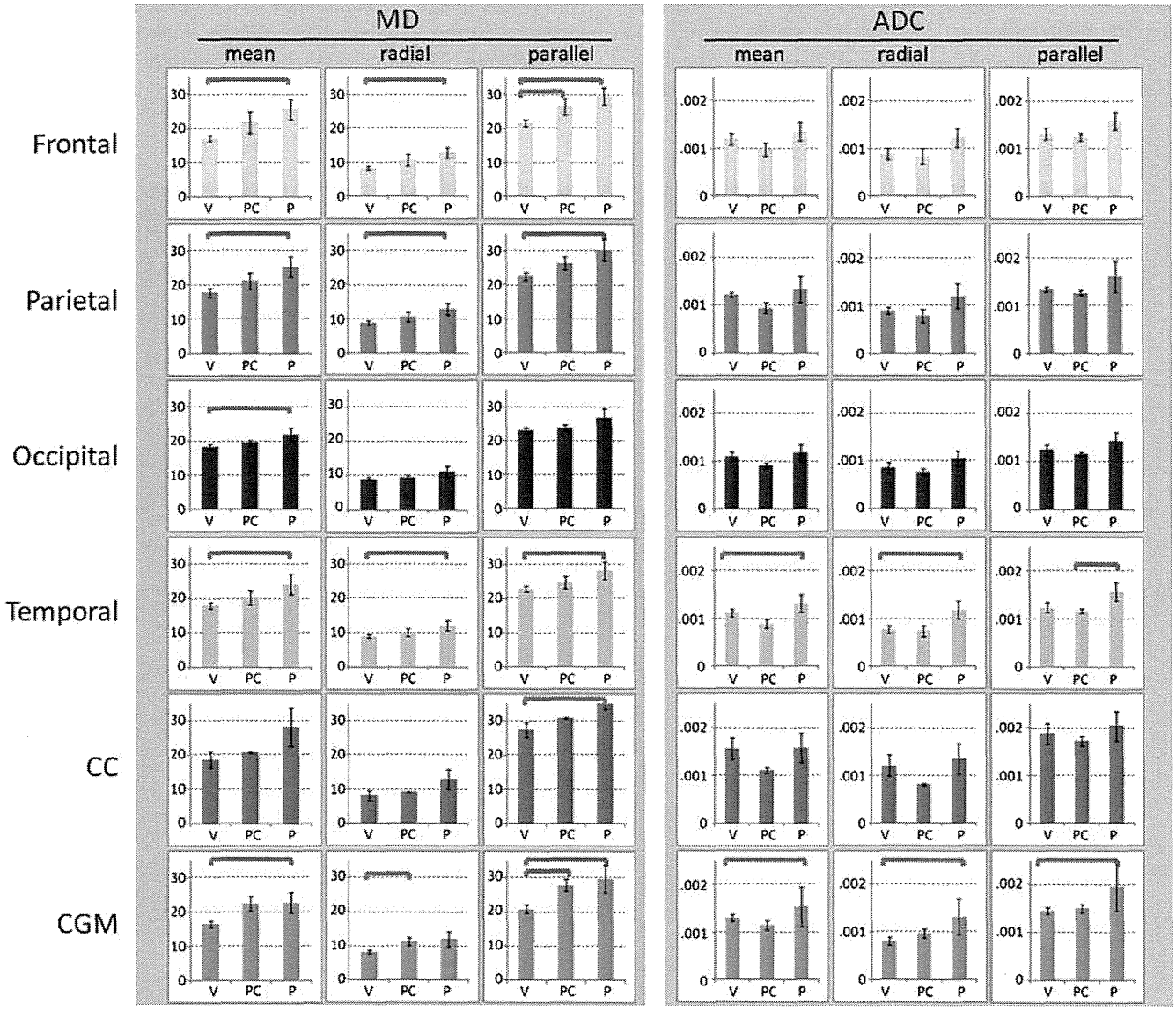

Fig. 2 Comparisons of normal volunteers (*V*), preclinical CADASIL patients (*PC*), and CADASIL patients (*P*). Substantial differences are noted in various locations, and the differences between normal and preclinical patients are most apparent using minimum mean displacement (*MD*) maps. *Frontal* frontal lobe, *Parietal* parietal lobe, *Occipital* occipital lobe, *Temporal* temporal lobe; *CC* corpus callosum; *CGM* central gray matter

calculated, and these values were used to represent the MD [14]. After this calculation, a tensor analysis was performed on MD for each voxel. The radial and parallel components of this tensor (MD_{radial} and $MD_{parallel}$) were also calculated. The ADC and the radial/parallel components of ADC (ADC_{radial} and $ADC_{parallel}$) were calculated from $b=0$ and $b=1{,}000$ s/mm^2.

ROI analysis

Region of interest (ROI) analysis was performed using manually segmented white matter of four lobes (e.g., frontal, parietal, occipital, and temporal lobes), corpus callosum, and central gray matter (Fig. 1). The ROI was defined on each subject by a single operator (KY) trained in neuroanatomy and neuroradiology. The patient's status was blinded when drawing these ROIs on the $b=0$ images. Signal-to-noise ratio was calculated by combining these ROIs with the denominator from the background ROI taken at the surrounding air of the head.

Statistics

Comparisons were performed using Student's t test (Matlab; The Mathworks, Natick, MA, USA) with Bonferroni corrections. The correlation was evaluated as significant for the P values of <0.005 for the comparison between the patients and healthy subjects and P values of <0.007 for the comparison between the preclinical (PC) subjects.

Visual assessment

Visual assessments of the images were carried out to further characterize the acquired maps of both normal volunteers and patients. This was done by the primary investigator (KY) of this study.

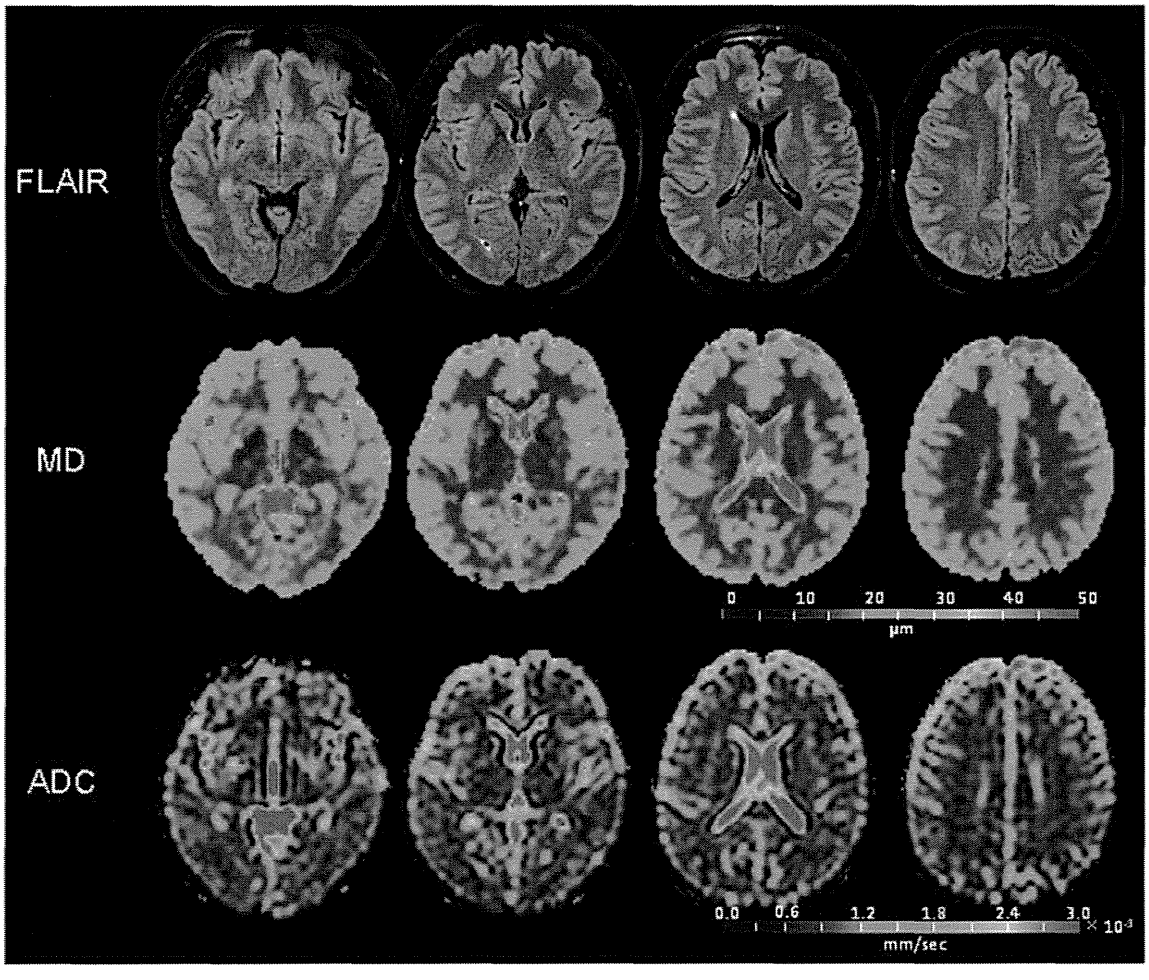

Fig. 3 Representative images from a normal volunteer. This is a 28-year-old man who volunteered to undergo the q-space imaging experiment. Note that, on the MD maps, there is clear definition between the cerebral cortex and underlying white matter. This is in contrast with the ADC maps that do not show a clear difference between the two structures

Results

ROI analysis

q-Space imaging was successfully carried out in all patients and volunteers, and the MD and ADC maps were generated from these data sets. The average signal-to-noise ratios (SNRs) for b=1,000 and b=10,000 were 16.3 and 9.1, respectively. The ROI analyses of these maps revealed substantial differences between the normal volunteers (V) and CADASIL patients (P) (Fig. 2). Statistically significant differences were noted at wider areas of the brain using q-space imaging than the ADC maps.

Some differences were also noted between the normal volunteers (V) and preclinical (PC) patients on MD_{radial} and $MD_{parallel}$. These differences were noted in the frontal white matter and central gray matters (CGM). Differences between the preclinical (PC) and symptomatic CADASIL patients (P) were noted in the temporal white matters on the ADC map (i.e., $ADC_{parallel}$) but not on MD maps.

Visual assessment

The MD maps of normal volunteers were characterized by white matter with uniformly low MD below 20 μm, represented by the blue color (Fig. 3). The cerebral cortex, on the other hand, had higher MD (shown by green color) with relatively well-defined contrast between the cortex and underlying white matter. This gray/white contrast was not clear on the ADC maps. The mean diffusivity of CGM was similar to the surrounding white matter.

Visual assessment of the MD maps on preclinical CADASIL (Fig. 4) and CADASIL patients (Fig. 5) revealed that there was a substantial increase in MD of the white matter in widespread areas. The white matter damage was readily recognizable on MD maps even in the preclinical stage.

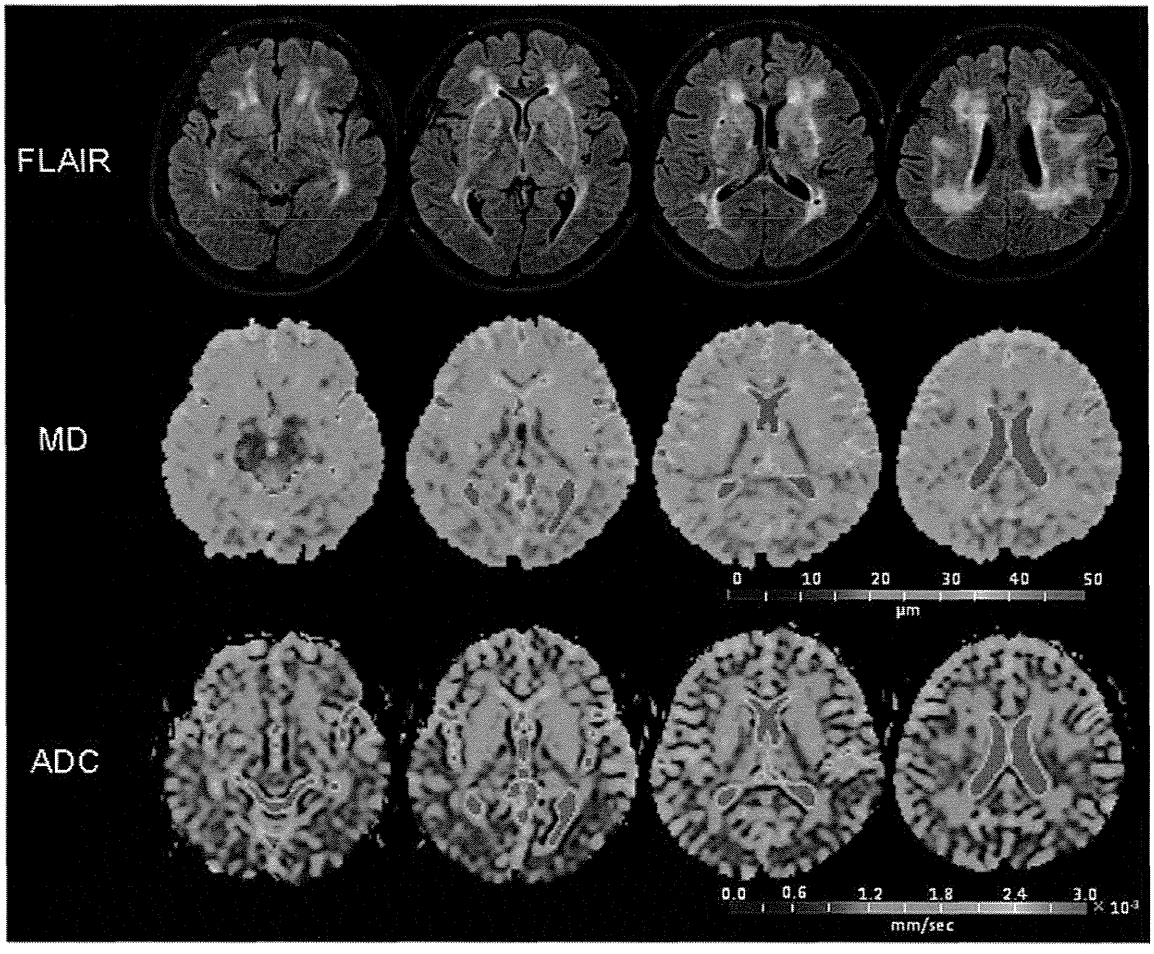

Fig. 4 Representative case of preclinical CADASIL. This is a 54-year-old man with CADASIL. The white matter damage is already apparent on the MD and ADC maps. Sparing of the U-fibers is also evident in some parts of the brain. Note that the posterior parts of the brain, including the occipital lobes, are relatively spared when compared with the other parts of brain. This trend of occipital lobe sparing is more clearly noted on the MD maps than the FLAIR

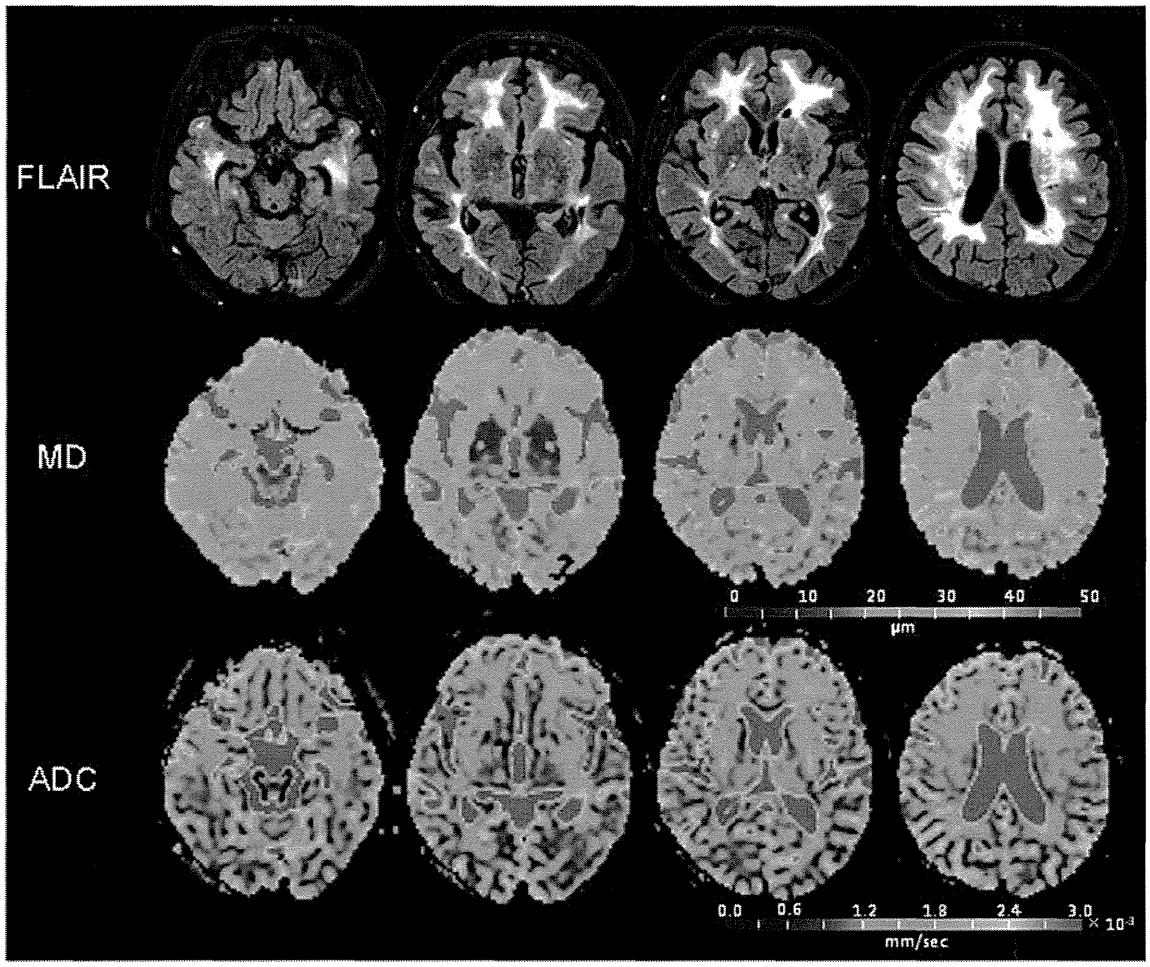

Fig. 5 Representative case of CADASIL. This is a 76-year-old man with full-blown CADASIL. The MD maps of q-space imaging reveal remarkable differences in the appearance of the white matter when compared with the normal volunteer and the preclinical case (Figs. 3 and 4). Sparing of the U-fibers is also evident in some parts of the brain, especially on ADC maps

There was also a trend for slight occipital lobe sparing, which was most apparent on MD maps even compared with the FLAIR.

Discussion

The results of the present study demonstrated that, using the q-space approach, the white matter damage in CADASIL patients could be readily visualized. Especially important could be the fact that it enables the observation of the earliest stage of neuronal damage. This implies the potential role of q-space imaging in assessing disease progression in preclinical patients. Preferential involvement of the fronto-parietal regions in the preclinical stage has been pointed out previously using MR imaging techniques, including MR spectroscopy and volumetric measurements [21]. This is in keeping with our ROI measurements.

In addition to these white matter regions, CGM was also severely affected already in the preclinical stage. It is well known from histological studies that the vessels most affected in CADASIL are the leptomeningeal and lenticulostriate arteries [22, 23]. Thus, the preferential involvement of the CGM in the present study was anticipated. It may be also noteworthy that despite such substantial changes at the CGM on q-space imaging, hyperintensity on FLAIR was not overt in some of the cases. For instance, as illustrated in Fig. 5, this particular CADASIL patient did not have significant hyperintensity at the thalami on FLAIR (Fig. 5). This superior sensitivity of q-space imaging to the CGM damages may be the potential advantage of this technique.

Since the q-space imaging technique appeared to be most sensitive to the early changes in the frontal lobes and CGM, these regions can be considered the potential target zones for monitoring the effect of future medical interventions. In order to test the potential role of q-space imaging as a monitoring tool, we are currently performing a longitudinal follow-up on our CADASIL population.

Degree of disease progression was examined by comparing the preclinical (PC) to symptomatic patients (P), as